

## Supporting Information

# Flexible Garnet Solid-State Electrolyte Membranes Enabled by Tile and Grout Design

Hua Xie<sup>1a</sup>, Yinhua Bao<sup>2a</sup>, Jian Cheng<sup>2</sup>, Chengwei Wang<sup>1</sup>, Emily M. Hitz<sup>1</sup>, Chunpeng Yang<sup>1</sup>, Zhiqiang Liang<sup>1</sup>, Yubing Zhou<sup>1</sup>, Shuaiming He<sup>1</sup>, Teng Li<sup>2\*</sup>, Liangbing Hu<sup>1\*</sup>

1. Department of Materials Science and Engineering, University of Maryland, College Park, Maryland, 20742
2. Department of Mechanical Engineering, University of Maryland, College Park, Maryland, 20742

\* Email: [binghu@umd.edu](mailto:binghu@umd.edu) [lit@umd.edu](mailto:lit@umd.edu)

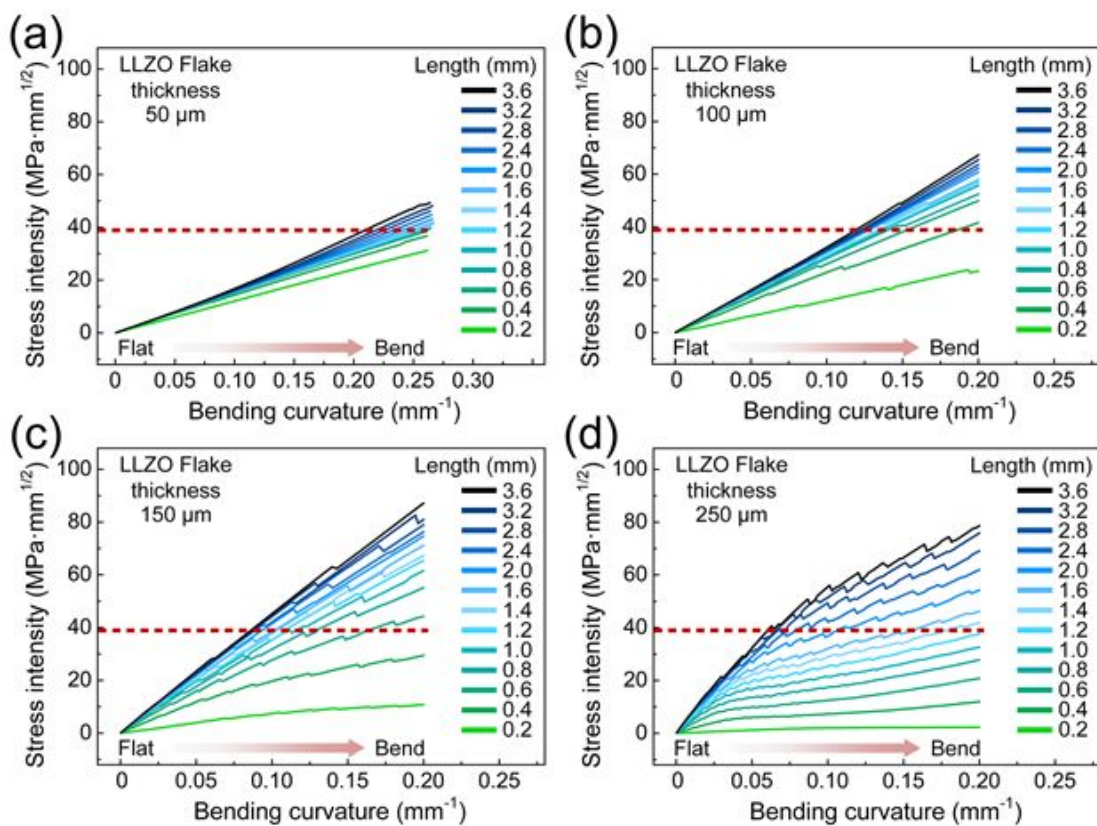


**Figure S1.** The relationship between stress intensity and bending curvature in LLZO chips of different lengths (from 0.2 to 3.6 mm) and thicknesses, including (a) 50 μm, (b) 100 μm, (c) 150 μm, and (d) 250 μm thick.

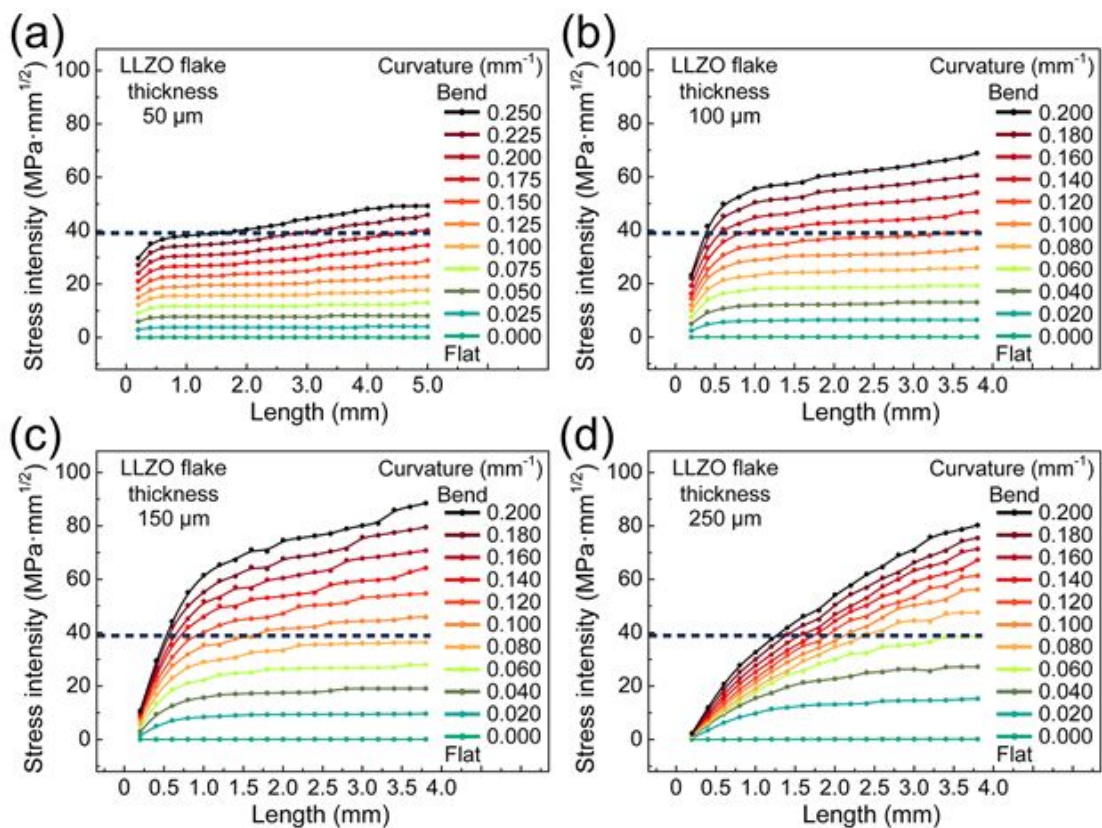


**Figure S2.** The relationship between stress intensity and chip length under different bending curvatures (from 0.0 to 0.25  $\text{mm}^{-1}$ ) in LLZO chips of different thicknesses, including (a) 50  $\mu\text{m}$ , (b) 100  $\mu\text{m}$ , (c) 150  $\mu\text{m}$ , and (d) 250  $\mu\text{m}$  thick.

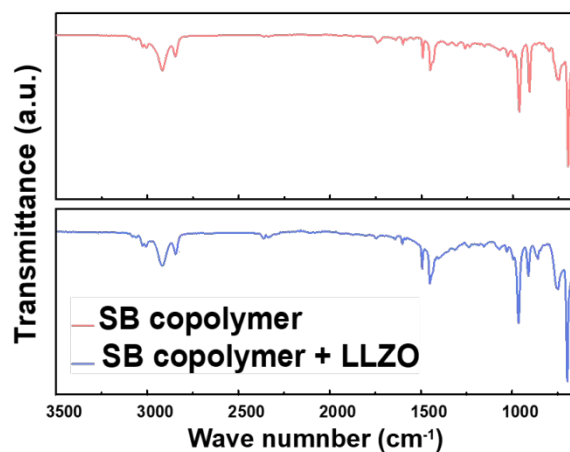


**Figure S3.** FTIR of the SBC and electrolyte membrane from 3250  $\text{cm}^{-1}$  to 640  $\text{cm}^{-1}$ .

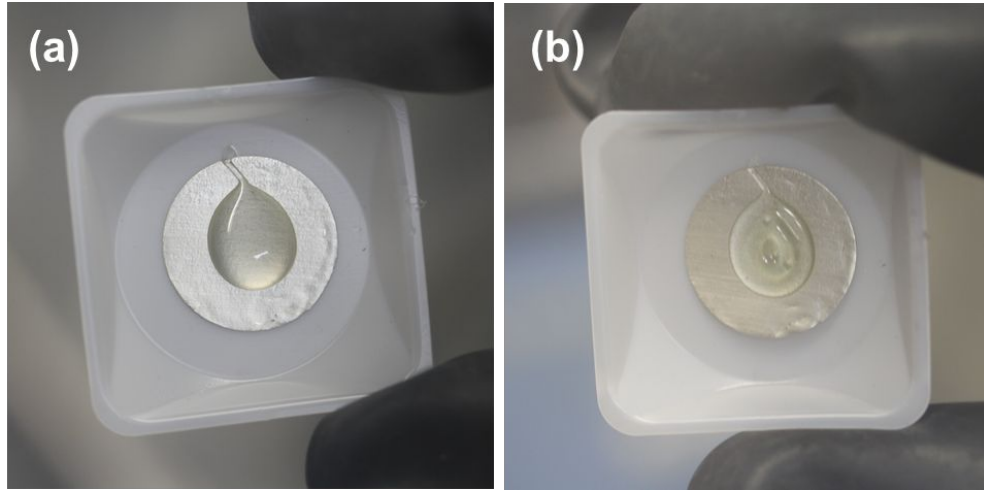


**Figure S4.** The stability test of the liquid SBC ink with Li. (a) The Li metal and the SBC ink in contact. (b) The lack of change in the appearance of either material indicates their good co-stability after the SBC had completely cured (48 h).

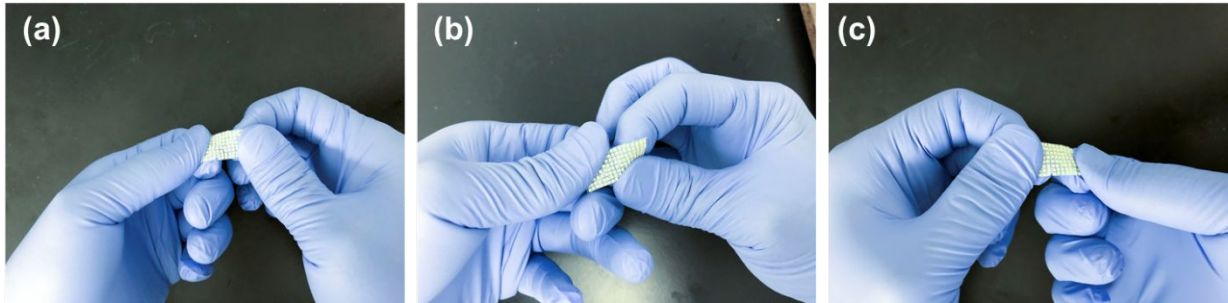


**Figure S5.** The stretchability of the composite electrolyte membrane

### Detailed finite elemental analysis (FEA) method

In the LLZO membrane breaking simulation process, LLZO chips were under bending state due to the constraints. We modeled a single LLZO chip bending process through a standard analysis in ABAQUS 6.13. To determine the critical breaking length of the LLZO chips, four different thicknesses of LLZO chips (50  $\mu\text{m}$ , 100  $\mu\text{m}$ , 150  $\mu\text{m}$ , 200  $\mu\text{m}$ , 250  $\mu\text{m}$ ) were considered. For each thickness, a series of LLZO chips with different lengths from 0.2 mm to 3.6 mm were

adopted in the modeling. The geometric parameters of the LLZO chips with different lengths and thicknesses are shown in Table S1.

**Table S1. Geometric parameters of the LLZO chip used in the FEA modeling**

Models		LLZO chip length (mm)												
		0.2	0.4	0.6	0.8	1.0	1.2	1.4	1.6	2.0	2.4	2.8	3.2	3.6
LLZO chip Thickness (μm)	100	1-1	1-2	1-3	1-4	1-5	1-6	1-7	1-8	1-9	1-10	1-11	1-12	1-13
	150	2-1	2-2	2-3	2-4	2-5	2-6	2-7	2-8	2-9	2-10	2-11	2-12	2-13
	200	3-1	3-2	3-3	3-4	3-5	3-6	3-7	3-8	3-9	3-10	3-11	3-12	3-13
	250	4-1	4-2	4-3	4-4	4-5	4-6	4-7	4-8	4-9	4-10	4-11	4-12	4-13

These 2D models were analyzed at the plain strain condition. The LLZO chips were simplified as elastic materials. The mechanical parameters are shown in Table S2.

**Table S2. Parameters used in the FEA modeling**

Parameters	Values
$E_{\text{LLZO}}$ , Young's Modulus of LLZO <sup>[1]</sup>	150 GPa
$\nu_{\text{LLZO}}$ , Poisson ratio of LLZO <sup>[2]</sup>	0.26
$K_{\text{IC}}$ LLZO Fracture toughness	39.528 $\text{MPa}\cdot\text{mm}^{1/2}$

A displacement load was applied on the two sides of the LLZO chip to model the bending process. A notch with a depth of 1.8  $\mu\text{m}$  was introduced in the middle position on the top surface of the LLZO chip for calculating the stress intensity. The bending curvature was calculated based on the displacement load. When the simulated stress intensity exceeded the LLZO fracture

toughness<sup>[3]</sup>  $K_{IC}$ , the surface notch started to crack. Based on this criterion, the relationship among the critical side lengths of the LLZO chip, the bending curvature (bending radius), and the chip thickness was determined.

### Supporting References

- [1] S. Yu, R. D. Schmidt, R. Garcia-Mendez, E. Herbert, N. J. Dudney, J. B. Wolfenstine, J. Sakamoto, D. J. Siegel, *Chem Mater* **2015**, 28, 197.
- [2] Z. Deng, Z. Wang, I. Chu, J. Luo, S. P. Ong, *J Electrochem Soc* **2016**, 163, A67.
- [3] J. Wolfenstine, H. Jo, Y. Cho, I. N. David, P. Askeland, E. D. Case, H. Kim, H. Choe, J. Sakamoto, *Mater Lett* **2013**, 96, 117.